Simulations Explain the Swelling Behavior of Hydrogels with Alternating Neutral and Weakly Acidic Blocks

David Beyer,[†] Peter Košovan,[*,‡] and Christian Holm[*,†]

†*Institute for Computational Physics, University of Stuttgart, D-70569 Stuttgart, Germany*

‡*Department of Physical and Macromolecular Chemistry, Charles University, Prague, Czechia*

E-mail: peter.kosovan@natur.cuni.cz; holm@icp.uni-stuttgart.de

[*]corresponding author

Abstract

We used computer simulations to study the equilibrium swelling of weak (pH-responsive) polyelectrolyte hydrogels as a function of pH and salt concentration in a supernatant solution. Our simulations were designed to represent recently synthesized gels composed of tetrapoly(acrylic acid) and tetrapoly(ethylene glycol) stars. To model the ionization equilibrium of the weak acid groups and the exchange of small ions with the reservoir, we applied the recently developed Grand-Reaction Monte-Carlo method. We showed that the ionization of these gels as a function of the pH significantly deviates from the ideal Henderson-Hasselbalch equation due to two main contributions: (1) electrostatic interactions and (2) Donnan partitioning of small ions. The first contribution dominates in the gels composed of alternating neutral and acidic blocks, contrasting with our previous observations that both contributions are comparably strong in hydrogels composed of homogeneously distributed weak acid groups.

We also critically examined the counterion condensation argument, previously invoked to explain why the experimentally observed swelling was lower than predicted by theory. Thus, a detailed analysis of the simulations allowed us to understand which of the above effects dominates in different systems and why, thereby allowing us to identify the correct physical origin of the deviations from ideal swelling. Such an understanding is important not only for correctly interpreting experimental measurements but also for designing polyelectrolyte gels tailored to exhibit specific swelling response to pH and salt concentration.

1 Introduction

Polyelectrolyte hydrogels are charged polymer networks formed by crosslinking of polyelectrolyte chains. The term "weak" polyelectrolyte hydrogels refers to the weakly acidic or weakly basic nature of the polyelectrolytes forming the hydrogels. Consequently, ionization states of weak polyelectrolyte hydrogels can vary from neutral to fully charged, depending on the pH value. One of the key features of polyelectrolyte hydrogels is their ability to swell by absorbing water, thereby increasing their volume up to a thousand times the volume of the dry gel. The enormous swelling ability of polyelectrolyte hydrogels is exploited in their application as superabsorbers in baby diapers, hygiene products or in agriculture.[1] Other applications, which have been proposed recently, include the desalination of salt water[2] and targeted drug-delivery.[3–7]

The swelling of polyelectrolyte hydrogels is predominantly determined by the osmotic pressure of the (counter-)ions as well as by the electrostatic repulsion of charged monomers and is thus strongly influenced by the degree of charging of the polyelectrolyte network. It is further modulated by other parameters, such as the salt concentration, counterion valency, density of crosslinking, or topology of the network. Because the charge state of weak polyelectrolyte hydrogels depends on the pH, a change in the pH is reflected by concomitant changes in the gel swelling. Qualitatively, the swelling response of weak polyelectrolyte hydrogels to changes in the pH is well known from

numerous experimental studies, e.g. Refs.[8–10] and understood from theories.[11–13] In brief, the swelling of a weak polyacid gel typically increases with the pH at a fixed salt concentration. This increase in swelling typically occurs at a pH which is about 2 units higher than $\mathrm{p}K_\mathrm{A}$ of the parent monomer, indicating that the ionization of the gel is lower than the ideal one, calculated using the Henderson-Hasselbalch equation

$$\alpha = \frac{1}{1 + 10^{\mathrm{p}K_\mathrm{A} - \mathrm{pH}}}. \tag{1}$$

In addition to that, an increase in the salt concentration at a fixed pH reduces the gel swelling. Although theoretical predictions qualitatively explain the experimentally observed changes in gel swelling as a function of pH, it is difficult to tell whether they correctly relate it to changes in the degree of charging of the gel because the latter quantity is not directly accessible from experiments.

To obtain a direct link between the microscopic structure of a hydrogel and its macroscopically observed properties, one can employ molecular simulations. Simulation models typically assume a regular, monodisperse network structure which allows one to consider a unit cell of the network. Periodic boundary conditions then ensure that the simulated system forms a quasi-infinite network. Particle-based simulations of hydrogels with all-atom resolution would be prohibitively expensive because of the required system sizes (tens of nm) and related relaxation times (microseconds and beyond). Therefore, coarse-grained models in implicit solvent are commonly employed to simulate such systems. In these models monomers are represented as effective particles while the solvent is included only implicitly as a dielectric continuum. On the coarse-grained level, some chemical details are neglected, while the model still accounts for the network connectivity, fluctuations in its structure, steric repulsion, and electrostatic interactions. Strong polyelectrolyte hydrogels with fixed charges have been simulated in this way already two decades ago.[14–21] However, the simulation of acid-base equilibria in weak polyelectrolyte hydrogels has become feasible only recently with the development of the Grand-Reaction Monte-Carlo (G-RxMC) method.[22] In our recent

simulation,[13] we have shown that the suppressed ionization in weak polyelectrolyte hydrogels can be explained by a synergistic action of two effects: (1) direct electrostatic repulsion between nearby ionized groups in the gel, termed the *polyelectrolyte effect* and (2) Donnan partitioning of ions which makes the pH inside the gel different from the supernatant solution, termed the *Donnan effect*. Thus, the current state of the art in the simulation methods allows us to predict the swelling of weak polyelectrolyte gels and compare these predictions with experiments, while simultaneously avoiding some approximations which are necessary to develop a phenomenological thermodynamic theory. However, until now a direct comparison of simulations results obtained using this new approach with experimental results is still lacking.

In general, comparing simulation predictions of hydrogel swelling to experiments is a challenge, because simulations typically assume a regular network structure, whereas most hydrogels are synthesized as irregular networks, containing a broad distribution of strand lengths. Therefore, it is not clear how the average degree of crosslinking, which is typically used to characterize real experimental networks, should be mapped to the strand length of the perfect network used in simulations. Some 15 years ago, Sakai et al. synthesized very regular and monodisperse networks with diamond-like topology by interlinking tetra-PEG stars with mutually reactive termini.[23] Recently, Tang et.al. extended this work by linking tetra-PAA and tetra-PEG stars,[10] yielding weak polyelectrolyte hydrogels with a regular diamond-like structure, composed of alternating neutral poly(ethyelenglycol) (PEG) and weakly acidic poly(acrylic acid) (PAA) blocks. Simultaneously, they investigated swelling properties of these networks at various values of pH and salt concentrations, thus providing a set of experimental results suitable for a direct comparison with theoretical models.

Tang et al.[10] also proposed a theoretical model which described the observed trends in the swelling of their gels as a function of pH and salt concentration. Their model was based on a mean-field approximation, estimating various contributions to the free energy and finding the swelling ratio of the gel which minimized the free energy as a function of the pH and salt concentration in the reservoir. Similar to the traditional

treatment of Flory and Rehner,[11] Tang et al. accounted for the elastic stretching of the chains, for the entropy of mixing and for the osmotic pressure of the ions. To calculate the number of counterions, they calculated the degree of ionization from the Henderson-Hasselbalch equation, coupled to the Donnan partitioning of H^+ ions to account for the Donnan effect. To include the polyelectrolyte effect, they determined experimentally the effective pK_A of free stars in solution and used this effective pK_A as the input for the Henderson-Hasselbalch equation.

Without further modifications, the model of Tang et al.[10] predicted that the gel should swell about 10 times more than they observed experimentally. To compensate for this overestimated swelling, they further invoked the Manning condensation of counterions,[24] using an effective renormalized charge

$$q^{\text{eff}}(\text{pH}) = \frac{q(\text{pH})}{\xi} = \frac{\alpha(\text{pH})q_{\text{max}}}{\xi} \quad \text{for} \quad \xi > 1, \tag{2}$$

where q is the bare charge, calculated from the Henderson-Hasselbalch equation, and q_{max} is the maximum attainable charge at $\alpha = 1$. The Manning parameter ξ determines the line charge density, i.e. the number of elementary charges per Bjerrum length λ_{B}. It can be expressed as

$$\xi(\text{pH}) = \frac{\lambda_{\text{B}}}{b} = \frac{\lambda_{\text{B}}\alpha(\text{pH})}{b_0}, \tag{3}$$

where b is the distance between the neighbouring charged groups. For the second equality, we employed the approximation $b = b_0/\alpha(\text{pH})$, where b_0 is the distance between neighbouring ionizable groups on the weak polyelectrolyte. This model assumes that if the bare charge on the polyelectrolyte exceeds the threshold of one charge per Bjerrum length ($\xi = 1$), then some counterions condense to yield an effective charge equal to the threshold value.

This renormalization seems plausible at first glance, however, a closer inspection reveals an inconsistency: The method used by Tang et al. to calculate $\alpha(\text{pH})$ (Eq.25 of Ref.[10]) accounts only for the polyelectrolyte effect, while neglecting the Donnan

effect on the ionization. Therefore, the value of α(pH) they used for renormalizing the charge was much higher than α(pH) used for calculating the gel swelling, because the latter included also the Donnan effect. Furthermore, the two-state model is a simplified description which is only valid for an infinitely long charged rod in the absence of salt. It has to be modified to correctly represent finite, flexible chains in the presence of salt [25] and it is not clear whether it can be applied to star-like polyelectrolytes with rather short arms. Therefore, although the charge renormalization used by Tang et al. [10] yields theoretical swelling curves that fit the experimental data better than without renormalization, it remains unclear whether this renormalization attributes the correct molecular origin to these observations.

The available literature suggest that not only counterion condensation but also other effects might lead to significant deviations from the ideal theory, similar to those obtained by charge renormalization. Our previous simulations,[21] combined with the augmented theory of Katchalsky and Michaeli [12], have shown that electrostatic interactions suppress the Donnan partitioning of small ions, thereby reducing the osmotic pressure and concomitantly reducing the gel swelling. Furthermore, in the same study we showed that the Gaussian approximation for the chain stretching tends to overestimate the swelling of polyelectrolyte hydrogels, predicting that the gel strands extend beyond their contour length even if the gels are only moderately charged. Next, the assumption of affine deformation works reasonably only for highly swollen gels with a homogeneous distribution of charges, whereas it fails for less charged gels, as soon as the gel strands are not sufficiently stretched.[21] Thus, one should expect that the affine deformation is not applicable to gels with alternating neutral and charged blocks because the neutral blocks stretch much less than the charged ones. By accounting for these effects, one should obtain swelling ratios of the gel which are lower than from the ideal theory, similar to what one obtains after renormalizing the charge.

Our goal in the current work is to provide simulation results, which could be confronted theoretical predictions of gel swelling as a function of pH and salt concentration, thereby allowing us to assess which approximations are physically meaningful and to

what extent they are applicable. Indeed, it has often been the case in polymer physics that simple phenomenological models, while in agreement with experimental data, attributed certain trends to the wrong origins. Our particle-based simulations allow for a detailed examination of different effects and their strength and thus enable assessing the validity of the proposed model. Simultaneously, by comparing our simulation predictions to the experiments on tetra-PEG-tetra-PAA gels Tang et al.[10], we provide the first direct comparison of such simulations with experiments on weak polyelectrolyte gels. This allows us not only to test the assumptions made in the phenomenological model employed in the original paper[10] but also to obtain insights into the microscopic gel structure, providing a molecular-level explanation of the experimentally observed trends in the swelling behaviour.

2 Model and Methods

2.1 Gel Model

To obtain the input parameters for our coarse-grained simulations, we estimated the number of segments as 115 per arm for neutral arms (PEG) and 62 per arm for acidic arms (PAA) from the experimentally determined molar masses of the stars.[10] In these experiments, the swelling of the hydrogel was investigated in equilibrium with an aqueous supernatant solutions at various pH and salt concentrations. In our simulations, we set pH and salt concentration of the supernatant solution (termed reservoir) and obtain the ionization and swelling degrees of the simulated gels as the outputs.

We used a coarse-grained gel model in periodic boundary conditions, similar to models used in our previous publications.[13,18,20,21] In this model, we consider the network to have a perfect, i.e. defect-free, diamond-like structure. For the current work, we retained this diamond-like structure but modified the gel topology with regards to chemical identity in order to mimic the experimentally studied gels composed of alternating acidic and neutral blocks.[10] The tetra-functional network contains two different

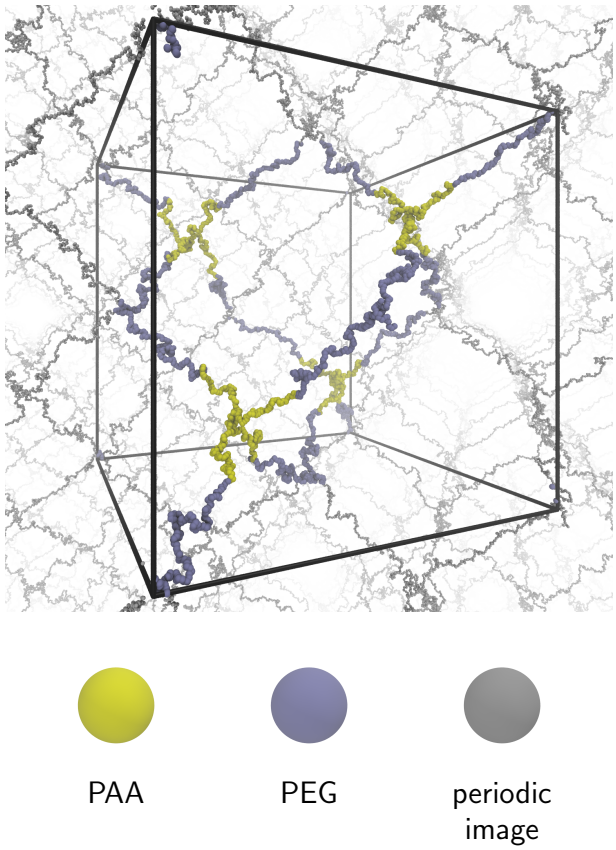

Figure 1: Snapshot of the periodic gel model. For clarity, small ions are not shown. The black box is the unit cell of the system. In order to enhance the visibility of the network structure, the shown box size is larger than the typical box size at swelling equilibrium.

kinds of nodes: neutral nodes from which four neutral arms extend and acidic nodes from which four acidic arms extend. Each arm is crosslinked to another arm of the opposite type, leading to a regular network structure with the same number of acidic and neutral nodes. The simulation snapshot in Figure 1 depicts a single unit cell of the model which contains a total of 8 nodes connected by 16 strands. Each strand between nodes consists of one block of 115 neutral segments and another block of 62 acidic segments. This unit cell is connected to other unit cells via periodic boundary conditions, creating an infinite network in which defects such as dangling arms and polydispersity of strands are neglected. The system is coupled to a reservoir characterized by the pH value and concentration of added salt which represents the buffer solutions used in the swelling experiments. Small ions can be exchanged between the system and the

reservoir whereas the polymer chains are present only in the system.

We employ a polymer model derived from the well-known generic Kremer-Grest model[26] and combine it with explicit ions and an implicit solvent, modeled as a dielectric characterized by ϵ, for the charge interactions. In this model, all particles (monomers and small ions) interact via a purely repulsive Lennard-Jones potential (Weeks-Chandler-Andersen or short WCA potential)[27] which models the excluded volume of the particles:

$$V_{\mathrm{WCA}}(r) = \begin{cases} 4\epsilon\left(\left(\frac{\sigma}{r}\right)^{12} - \left(\frac{\sigma}{r}\right)^{6}\right) + \epsilon & \text{if } r \leq 2^{\frac{1}{6}}\sigma \\ 0 & \text{if } r > 2^{\frac{1}{6}}\sigma. \end{cases} \tag{4}$$

We set the bead diameter to a value of $\sigma = 0.355\,\mathrm{nm}$ and the energy scale to $\epsilon = k_{\mathrm{B}}T$. In particular, we do not consider any monomer-specific interactions (i.e. hydrophobic interactions) and thus all different chemical species interact with a purely repulsive short-range interaction. The chemical bonds between neighbouring monomers are represented by finitely extensible nonlinear elastic (FENE) bonds[28]

$$V_{\mathrm{FENE}}(r) = \begin{cases} -\frac{k\Delta r_{\max}^2}{2}\ln\left(1 - \left(\frac{r-r_0}{\Delta r_{\max}}\right)^2\right) & \text{if } r \leq \Delta r_{\max} \\ \infty & \text{if } r > \Delta r_{\max}, \end{cases} \tag{5}$$

where we set the maximum extension of the bonds to $\Delta r_{\max} = 1.5\sigma$, the spring constant to $k = 30k_{\mathrm{B}}T/\sigma^2$, and $r_0 = 0$.

The electrostatic interactions between the explicit ions are described by the Coulomb potential

$$V_{\mathrm{Coulomb}}^{ij}(r) = \frac{\lambda_{\mathrm{B}}k_{\mathrm{B}}Tz_iz_j}{r} \tag{6}$$

with the ion valencies z_i. To account for the dielectric properties of the implicit solvent, we set the Bjerrum length $\lambda_{\mathrm{B}} = e^2/4\pi\epsilon k_{\mathrm{B}}T$ to a value of $\lambda_{\mathrm{B}} = 2\sigma = 7.1\,\text{Å}$ which corresponds to water at a temperature of $T \approx 300\,\mathrm{K}$. We employ the $\mathrm{P^3M}$ method[29]

to efficiently sum the long-range electrostatic forces and energies and set the relative error for the P^3M method to a value of 10^{-3}.[30,31]

2.2 Simulation Methods

To sample different conformations of the gel, we use the Langevin dynamics method with a friction coefficient of $\gamma = 1.0\,\tau^{-1}$, where $\tau = \sigma\,(m/k_{\mathrm{B}}T)^{1/2}$ is the Lennard-Jones unit of time.[32] The numerical integration is performed using the Velocity-Verlet integrator[32] with a time step of $\Delta t = 0.01\,\tau$. The particle mass m is irrelevant for equilibrium properties and for convenience, we set it to $m = 1.0$.

In addition to the sampling of different conformations at a fixed chemical composition of the gel, we also accounted for the dissociation equilibrium of the weak acid groups on the PAA blocks:

$$\mathrm{HA} \rightleftharpoons \mathrm{A}^- + \mathrm{H}^+. \tag{7}$$

with $\mathrm{p}K_{\mathrm{A}} = 4.25$ which corresponds to acrylic acid.

Furthermore, we also model the exchange of small ions between the gel and the the reservoir at given value of pH and salt concentration, represented by a set of virtual chemical reactions:

$$\emptyset \rightleftharpoons \mathrm{H}^+ + \mathrm{OH}^- \tag{8}$$

$$\emptyset \rightleftharpoons \mathrm{Na}^+ + \mathrm{Cl}^- \tag{9}$$

$$\emptyset \rightleftharpoons \mathrm{Na}^+ + \mathrm{OH}^- \tag{10}$$

$$\emptyset \rightleftharpoons \mathrm{H}^+ + \mathrm{Cl}^-. \tag{11}$$

The equilibrium constants of these reactions were derived from the desired concentrations of these species in the reservoir, as described in Ref.[33] To simulate these effects, we used the Grand-Reaction Monte-Carlo method (G-RxMC)[22]. All simulations were performed using version 4.1 of the open-source simulation software ESPResSo.[34] Full

details of the implementation and of the simulation protocol are provided in Ref.[33].

2.3 Simulation Protocol

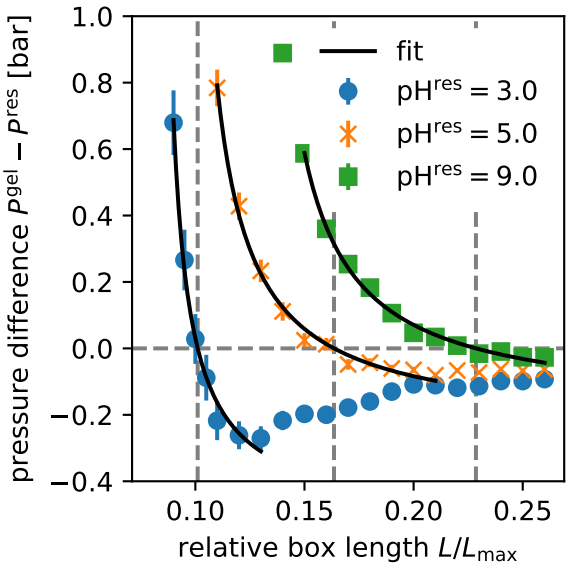

Figure 2: Plot of the pressure difference $P^{sys} - P^{res}$ as a function of the simulation box length L and for different values of pH^{res}. The shown curves correspond to a reservoir salt concentration of $c^{res}_{NaCl} = 10\,mM$. Error bars are included for all data points but are often smaller than the symbol size. Vertical lines indicate the equilibrium volumes determined from the fits. Analogous plots for all simulated parameters are available from Ref.[33]

The free swelling equilibrium between the gel and the supernatant solution (reservoir) is characterized by the following conditions: First, both phases have to be in an electrochemical equilibrium with respect to the small ions, i.e. $\overline{\mu}_i^{res} = \overline{\mu}_i^{sys}$ for $i = H^+, OH^-, Na^+, Cl^-$. This condition is automatically fulfilled by the G-RxMC method. Second, we require a mechanical equilibrium between the two phases, i.e. $P^{res} = P^{sys}$, which is equivalent to a minimization of the Helmholtz free energy of the (gel + reservoir) with respect to the gel volume. To fulfill the second condition, we used a simulation protocol similar to those employed in previous publications.[13,21] We simulated the system at different box lengths L and measure the pressure in each of these simulations as described in detail in Ref.[33] Using this simulation protocol, we obtained the pressure difference $\Delta P = P^{res} - P^{sys}$ as a function of the box length

L, as shown in Figure 2 for selected parameters of the simulated systems. Analogous pressure – box-length plots for all simulated parameters can be found in Ref.[33]

To determine the equilibrium box length L_{eq} and thus the equilibrium volume $V_{\mathrm{eq}} = L_{\mathrm{eq}}^3$, we fit the phenomenological function $f(L) = a + b/\tan(L - c)$ with fit parameters a, b and c to the pressure difference $\Delta P(L)$ near the zero crossing and calculate the intersection with the zero line. Although this fit function has no physical significance, it reasonably approximates the pressure curves near $P_{\mathrm{ext}} = 0$, as is demonstrated by examples of pressure-volume curves with the corresponding fits in Figure 2. After determining the simulation box length at the free swelling equilibrium, L_{eq}, we performed additional simulations with fixed box length L_{eq} in order to determine properties of the gels at free swelling equilibrium. When computing ensemble averages of the observables, we averaged over four independent simulation runs.

To quantify the swelling of the hydrogels, we define the volume-based swelling ratio

$$Q \equiv \frac{V}{V_{\mathrm{dry}}} \tag{12}$$

where $V_{\mathrm{dry}} = N_{\mathrm{beads}} \cdot \left(4\pi(\sigma/2)^3/3\right)/0.64$ is the volume of the dry gel, defined as the volume occupied by the N_{beads} monomers at maximum random packing fraction of hard spheres, 64%.

3 Results

3.1 Gel Swelling as a Function of pH and Salt Concentration

In Figure 3 we plot the volume-based swelling ratio as a function of pH in the reservoir, obtained from the simulations at various salt concentrations $c_{\mathrm{NaCl}}^{\mathrm{res}}$. The observed trend qualitatively agrees with the trends observed in earlier theoretical[11,12] and experimental[8,9] studies: The swelling ratio initially increases as the pH is increased, reaching

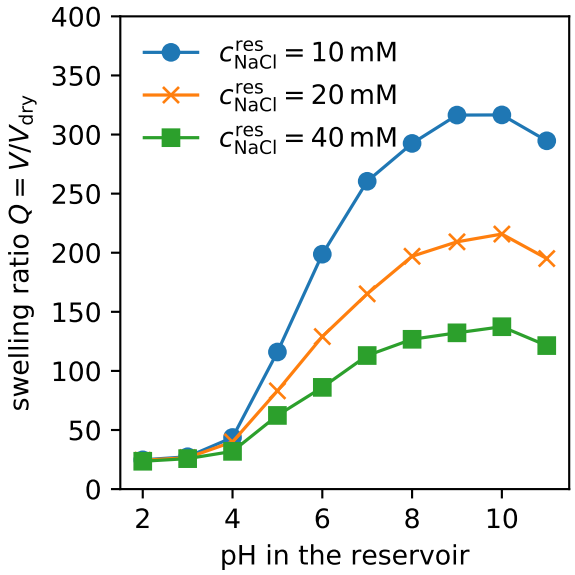

Figure 3: The equilibrium swelling ratio as a function of the reservoir pH as obtained from the simulations at various salt concentrations.

a plateau at $\mathrm{pH}^{\mathrm{res}} \gg \mathrm{p}K_{\mathrm{A}}$, which in our case occurs at $\mathrm{pH}^{\mathrm{res}} \approx 8$. This increase in the swelling ratio is due to two main contributions. Firstly, as the degree of ionization of the acid monomers increases with increasing pH, the number of counterions in the gel increases too, which in turn leads to an increase in the osmotic pressure, causing the gel to swell. Secondly, the increasing number of charges on the chains increases their mutual repulsion, thus also contributing to an increased swelling of the network. Furthermore, we observe that the swelling decreases as the salt concentration is increased at a fixed value of $\mathrm{pH}^{\mathrm{res}}$. Likewise, this trend can also be attributed to two main effects. On the one hand, an increase in the salt concentration decreases the osmotic pressure. On the other hand, an increase in the salt concentration also increases the screening of the electrostatic interaction, thereby reducing the repulsion between charged monomers.

In the next step, we compare our simulation results to the experimental measurements by Tang et al.[10]. Unfortunately, the *initial volume*, which was employed in the experiments to calculate the swelling ratio, cannot be calculated from the simulations. Therefore, we have chosen the maximum value of the swelling ratio to normalize the

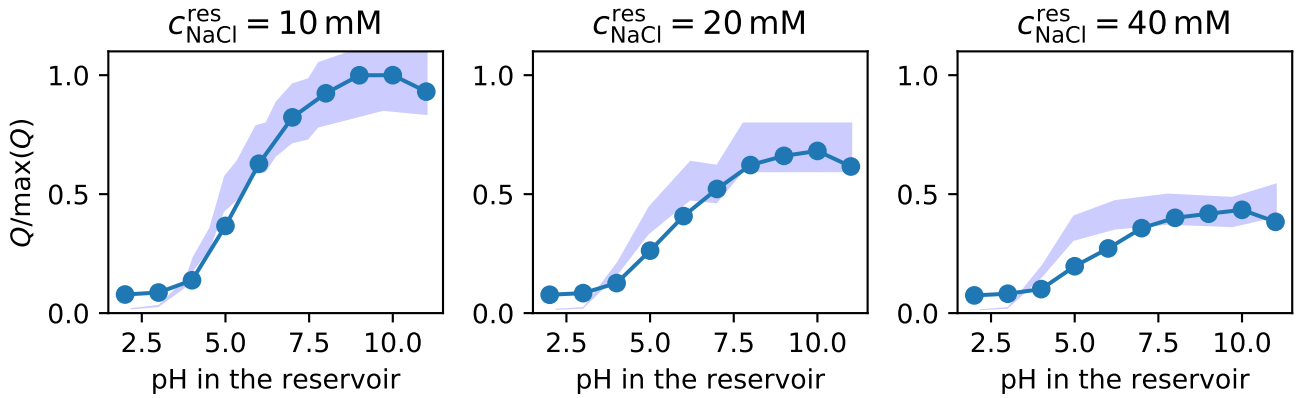

Figure 4: Comparison of the volume-based swelling ratio as a function of pH in the reservoir, determined from our simulations and experiments by Tang *et al*[10]. To ensure comparability, the data is normalized by the respective maximum values. The data points connected by lines represent the simulation results whereas the experimental results (including error bars) are represented by the shaded region.

measured swelling ratios,

$$\frac{Q}{\max(Q)} = \frac{V/V_{\mathrm{ref}}}{\max(V/V_{\mathrm{ref}})} = \frac{V}{\max(V)}.$$

With this normalization, the volumes in reference state cancel out, thus enabling a parameter-free comparison of swelling ratios determined from experiments and simulations, based on different reference states. Figure 4 shows that the simulated swelling ratios agree with the experiments for high and intermediate values of $\mathrm{pH}^{\mathrm{res}}$ and $c_{\mathrm{salt}}^{\mathrm{res}} < 40\,\mathrm{mM}$ whereas the agreement is not so good at the highest salt concentration, $c_{\mathrm{salt}}^{\mathrm{res}} = 40\,\mathrm{mM}$. At $\mathrm{pH}^{\mathrm{res}} \lesssim 4$, the simulations overestimate the swelling ratio, as compared to the experiments. We attribute these discrepancies to the lack of chemical specificity, especially any kind of attractive short-range interactions, in our coarse-grained model. Such contributions become important at low swelling of the gels because of the higher density of monomers. For instance, it is known that PAA is slightly hydrophobic, which may alter the behaviour at low degrees of ionization. Nevertheless, as long as the gel swelling is sufficiently high, so that electrostatic interactions dominate, our simulations well reproduce the experimental observations.

3.2 Ionization Degree of the Gels at Various pH Values and Salt Concentrations

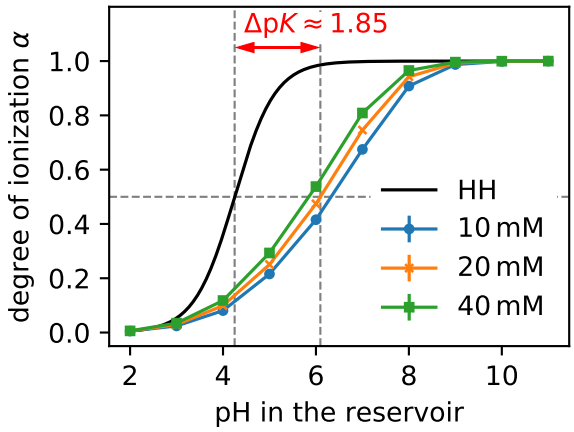

a)

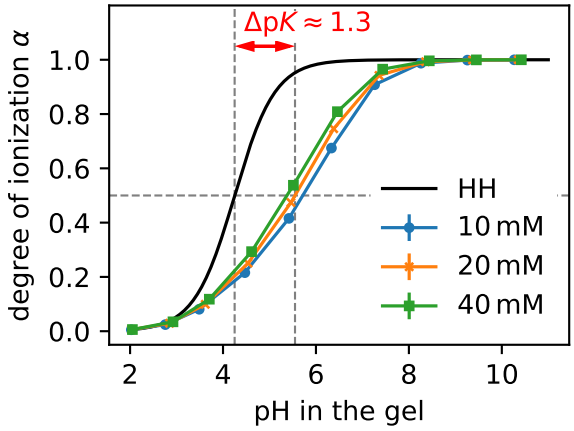

b)

Figure 5: Ionization degree of the gels at various values of the reservoir salt concentration $c^{\text{res}}_{\text{NaCl}}$: (a): as a function of the pH in the reservoir; (b): as a function of the pH inside the gel.

Intuitively, it is clear that a change in the swelling as a function of pH is coupled to changes in the degree of ionization, however, the latter is not directly accessible in experiments. Therefore, changes in the degree of ionization as a function of pH have been often inferred indirectly from the swelling response of the gels. In contrast with that, we can directly measure the degree of ionization of the gel in our simulations at the

swelling equilibrium. In Figure 5a, we observe that the degree of ionization of the gel as a function of pH in the reservoir significantly deviates from the ideal result, described by the Henderson-Hasselbalch equation. The simulated curves are shifted to higher values of $\mathrm{pH}^{\mathrm{res}}$, which can be interpreted as an increase in the effective $\mathrm{p}K_{\mathrm{A}}$ of the gel, as compared to the free monomers. This effective $\mathrm{p}K_{\mathrm{A}}$ is defined as the pH-value for which the gel acquires an ionization of $\alpha = 0.5$. For example, the gel attains a value of $\alpha = 0.5$ at $\mathrm{pH} \approx 6.1$, as compared to $\mathrm{pH} = 4.25$ for the ideal curve, thus corresponding to $\Delta\mathrm{p}K_{\mathrm{A}} \approx 1.85$. Alternatively, one may regard the ionization of the gel as being strongly suppressed compared to the Henderson-Hasselbalch result. In addition, the deviations of the simulation results from the ideal HH result decrease as the salt concentration in the reservoir is increased. In the preceding publication,[13] we have shown that these deviations can be caused by two different effects: 1. the "Donnan effect", caused by the unequal partitioning of H^+ between the gel and the reservoir, which leads to a difference of the pH inside the gel and in the reservoir; 2. the "polyelectrolyte effect", caused by the electrostatic repulsion between monomers along the same chain. Because the Donnan effect is solely due to the Donnan partitioning, it can also be observed in ideal gel models with Donnan partitioning. In contrast, the polyelectrolyte effect is purely a consequence of the electrostatic repulsion between nearby like-charged monomers. This repulsion increases the interaction energy, penalizing highly ionized states of the chains and thus effectively suppressing the ionization as compared to an ideal system. To quantitatively distinguish the influence of the two effects on the degree of ionization of the gel, we effectively subtract the Donnan effect by plotting the degree of ionization as a function of the pH inside the gel, which we approximate as[13]

$$\mathrm{pH}^{\mathrm{gel}} \approx \mathrm{pH}^{\mathrm{res}} - \log_{10}(c^{\mathrm{gel}}_{\mathrm{H}^+}/c^{\mathrm{res}}_{\mathrm{H}^+}) = \mathrm{pH}^{\mathrm{res}} - \log_{10}(c^{\mathrm{gel}}_{\mathrm{Na}^+}/c^{\mathrm{res}}_{\mathrm{Na}^+}). \tag{13}$$

In Figure 5b we show that the shift from the ideal curve becomes slightly smaller after subtracting the Donnan effect. All remaining deviations are solely due to the interactions, i.e. the poylelectrolyte effect. A comparison of Figure 5a and Figure 5b thus

reveals that the polyelectrolyte effect is the dominating contribution in the investigated system. This comparison contrasts with a similar comparison performed in our preceding publication on the swelling of weak polyelectrolyte hydrogels,[13] where we observed that the swelling is either dominated by the Donnan effect or both effects are comparable in magnitude. The only difference between our current simulations and those in the preceding study consists in the structure of the simulated gels. In the preceding work, all monomers in the gels were weakly acidic whereas in the current work the gel consists of weak polyacid stars connected by neutral (non-ionizable) stars, resulting in a structure composed of regularly alternating ionizable and non-ionizable blocks. Thus, our simulations show that the Donnan effect is suppressed while the polyelectrolyte effect is enhanced in the block-like gels, as compared to gels with homogeneously distributed ionizable groups.

3.3 Gel Structure

To understand how the block-like structure of the gels simulated in the current study affects the role of the Donnan and polyelectrolyte effect in their swelling, we investigate the gel structure by measuring the radii of gyration, R_{g}, of the neutral and acidic blocks. In Figure 6 we show that R_{g} of the neutral blocks increases only slightly as the degree of ionization is increased whereas R_{g} of the ionizable blocks increases by a factor of 2 as they become more charged upon an increase in the pH. Therefore, unlike the homogeneously ionizable gels which we simulated previously[13], our current gels, composed of alternating neutral and ionizable blocks, do not swell homogeneously as the pH is increased. In the current gels, the dominant contribution to swelling upon an increase in the pH comes from the ionizable blocks whereas the neutral blocks contribute only negligibly. This picture is further confirmed by Figure 7, showing simulation snapshots of the gels at low and high degrees of ionization, ($\alpha \approx 0$, pH $= 2$), and ($\alpha \approx 1$ pH $= 11$), respectively. The snapshots at low α confirm that both ionizable and neutral blocks attain similar conformations. In contrast, the snapshots at high α show that the acidic blocks are highly stretched and take up most of the volume

while the neutral blocks retain similar conformations as they had at low α. Therefore, the structure of the swollen block-like gel resembles a semidilute solution of star-like polyelectrolytes, loosely connected by flexible neutral chains.

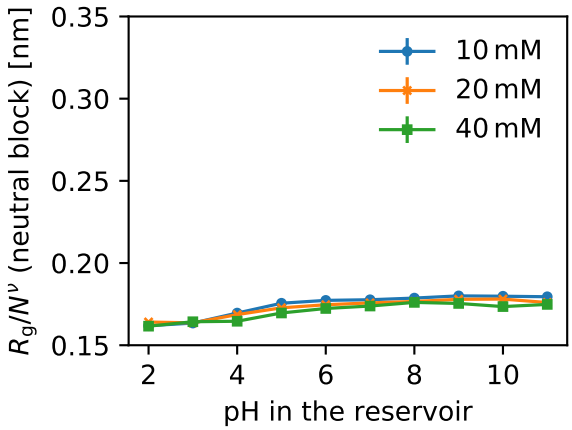

a)

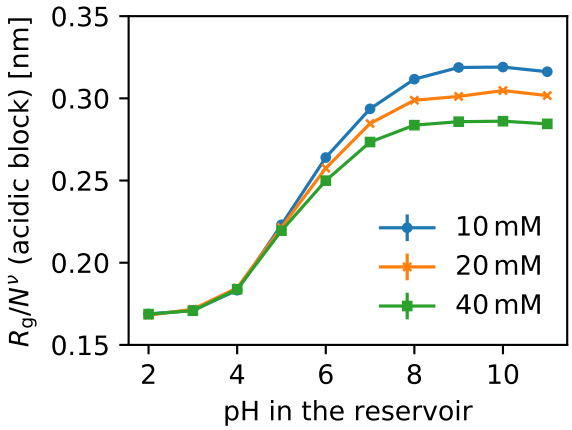

b)

Figure 6: Plots of the radii of gyration of neutral and acidic blocks as a function of the degree of ionization of the gel and for different salt concentrations $c^{\mathrm{res}}_{\mathrm{NaCl}}$ of the reservoir. The results have been normalized by the scaling law N^ν with $\nu = 0.588$ to make the neutral and acidic blocks of different lengths comparable.

This difference between homogeneously ionizable and block-like gels can be understood by recognizing that the electrostatic repulsion between charged acid monomers (polyelectrolyte effect) affects only the ionizable blocks whereas the osmotic pressure of counterions (Donnan effect) affects all segments of the gel, irrespective of their charge.

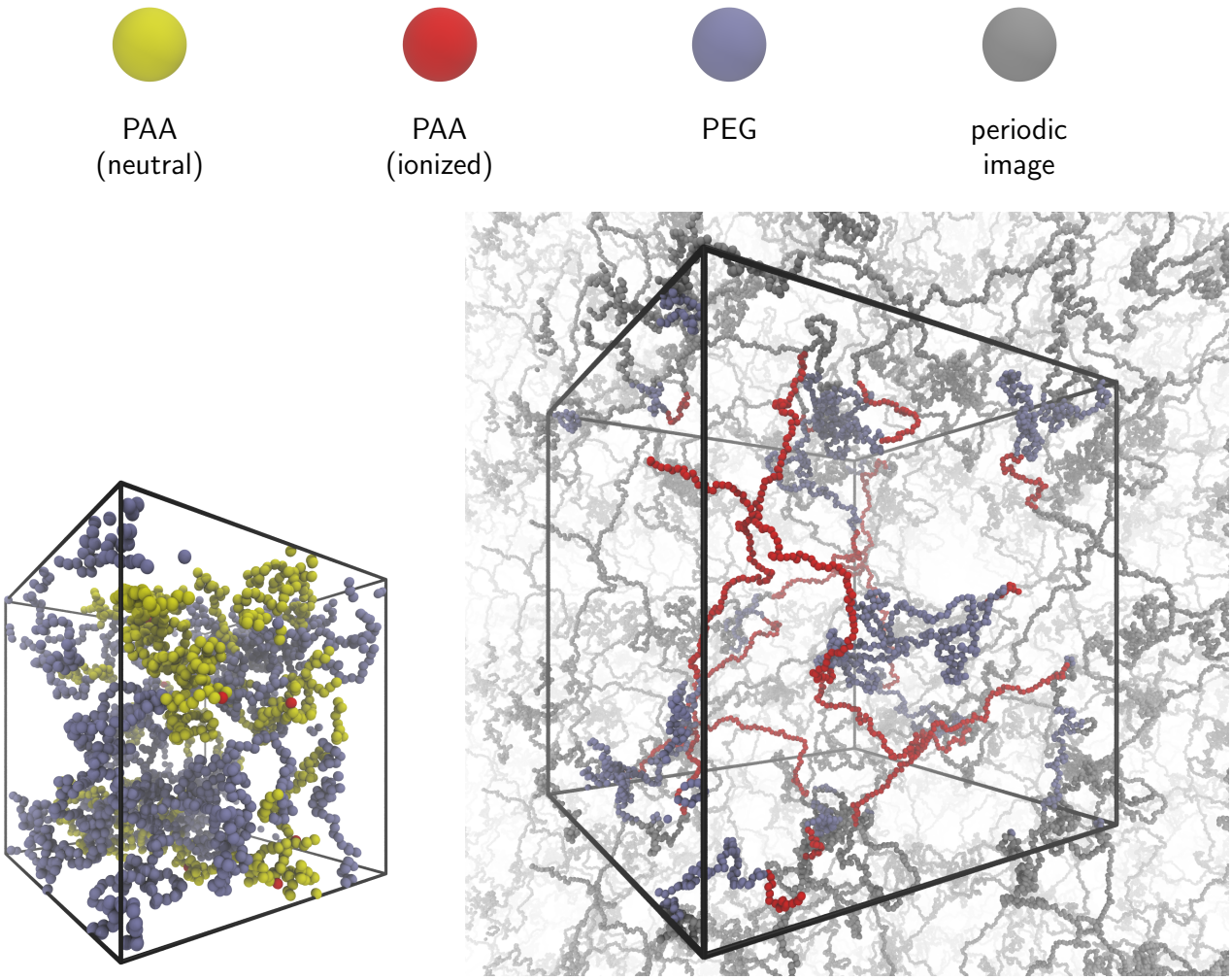

(a): $c_{\mathrm{NaCl}}^{\mathrm{res}} = 10\,\mathrm{mM}$, $\mathrm{pH}^{\mathrm{res}} = 2$, $\alpha \approx 0$

(b): $c_{\mathrm{NaCl}}^{\mathrm{res}} = 10\,\mathrm{mM}$, $\mathrm{pH}^{\mathrm{res}} = 11$, $\alpha \approx 1$

Figure 7: Simulation snapshots of the gel at $c_{\mathrm{NaCl}}^{\mathrm{res}} = 10\,\mathrm{mM}$ in the non-ionized state (panel a) and fully ionized state (panel b). For clarity, small ions have been omitted in both pictures and the periodic images around the primary simulation box are shown only in panel b. The boxes are not shown to scale; the magnification in panel a is greater than in panel b.

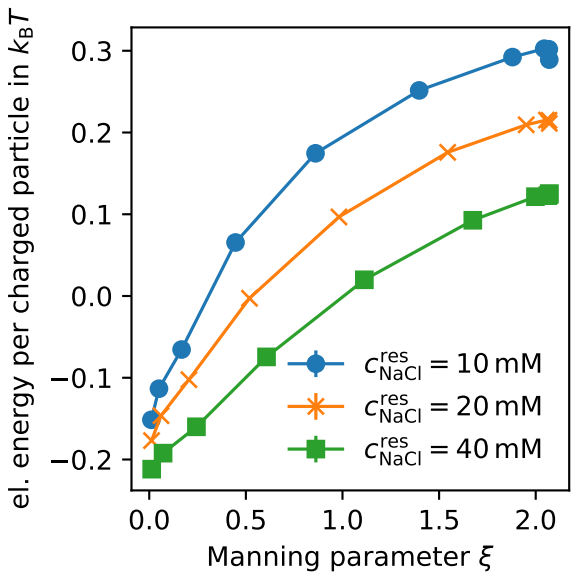

Figure 8: Mean electrostatic energy per charged particle as a function of the Manning parameter $\xi = \lambda_B / l_{charge}$ for different salt concentration c^{res}_{NaCl} of the reservoir.

Because of the block-like structure, the ionizable segments are kept closer to each other than in a gel with homogeneously distributed ionizable groups which occupies the same total volume. Therefore, the electrostatic repulsion in a block-like gel is greater than in an analogous homogeneously ionizable gel, making the polyelectrolyte effect stronger. On the contrary, while the ionizable segments are confined within the volume occupied by the ionized blocks, the total volume of the gel is greater because it includes the volume occupied by the neutral blocks. Therefore, the Donnan effect is suppressed in a block-like gel, as compared to an analogous homogeneously ionizable gel. Ultimately, the block-like structure of gels composed of alternating neutral and ionizable blocks causes that the electrostatic repulsion between the charged monomers is the dominant contribution causing deviations from the ideal swelling and ionization response to changes in the pH.

3.4 Probing for Counterion Condensation

In contrast to our explanations given before, Tang et al.[10] used arguments based on the Manning theory of counterion condensation[24,35] to theoretically rationalize why

their experiments yielded lower swelling than predicted by their theory. To settle the question if counterion condensation actually occurs in the present system and if the application of the Manning theory is justified, we probe our simulation results for various features of counterion condensation.

Theory predicts that counterion condensation on an infinite charged cylinder in the absence of added salt can be identified as a cusp at the critical Manning parameter $\xi_c = 1$ in the plot of the electrostatic energy per charged particle as a function of the Manning parameter.[36] For a finite and flexible polyelectrolyte chain, the transition is more gradual, which can be identified by a maximum in the same plot, as has been observed in computer simulations of weak polyelectrolytes.[37] In Figure 8 we show that in our gels the plot of the electrostatic energy per charged particle monotonically increases as a function of the Manning parameter, ξ. This happens irrespective of the salt concentration. While this behaviour indicates that counterion condensation does not occur in this system, it does not provide conclusive evidence yet, because the criterion is based on a prediction for a salt-free system.[36]

Alternatively, counterion condensation on a rod in the presence of salt can be characterized by two inflection points of the cumulative distribution function of counterions, $P(r)$, when plotted as a function of the logarithm of the distance to the rod.[25] In our simulations, $P(r)$ is given by

$$P(r) = \frac{\sum_i z_i \int_0^r \mathrm{d}r' p_i(r')}{\sum_i z_i N_i}, \tag{14}$$

where z_i is the valency of species i and $p_i(r)$ is the number density of ions of type i whose smallest distance to an acid monomer is given by r. $P(r)$ is normalized such that it approaches 1 far from the chain. Note that this criterion should only be applied in the limit of high ionization, when the chains attain rod-like conformations. In Figure 9, we plot $P(r)$ at different salt concentrations and $\mathrm{pH}^{\mathrm{res}} = 11$. Our gels are fully ionized at this pH, yielding the highest value of the Manning parameter which could be attained in our gels, $\xi \approx 2$, well above the critical value. In in Ref.[33] we

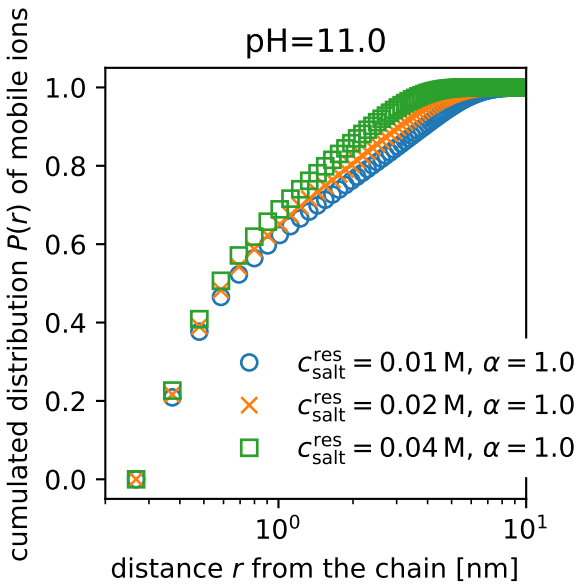

Figure 9: Cumulative distribution function of counters around charged segments of the gel, $P(r)$, as a function of the distance from the chain r (plotted on a logarithmic scale). The shown curves were obtained from simulations at $\text{pH}^{\text{res}} = 11$ (corresponding to $\xi \approx 2$) and various salt concentrations as indicated in the legend.

provided a detailed analysis of the first and second derivatives of the curves displayed in Figure 9, showing that in some cases two inflection points are indeed present if $\alpha \gtrsim 0.5$ which corresponds to $\xi \approx 1$ in our model. Thus, this alternative analysis indicates that some sort of counterion condensation may be present in the studied system if the degree of ionization is sufficiently high.

3.5 Comparison with the phenomenological model of Tang et al.

Based our analysis of the ionization response of the gels and quantification of the contributions due to the Donnan and the polyelectrolyte effect, we conclude that the phenomenological model of Tang et al.[10] approximately accounted for both these effects. They estimated semi-empirically the polyelectrolyte effect by determining the effective $\text{p}K_{\text{A}}$ of the free stars in solution from potentiometric titrations. However, in Ref.[33], (Figure S1) we show that the net charge calculated using the effective $\text{p}K_{\text{A}}$ as

the input of Henderson-Hasselbalch equation does not match very well with the net charge calculated directly from the potentiometric titration data by Tang et al.[10]. On the contrary, the net charge calculated from our simulations of star polyelectrolytes in solution very well matches the titration data points. This comparison *a posteriori* confirms that the parameters of our simulation model were chosen correctly to represent the real polyelectrolytes. The use of effective pK_{A} in combination with the HH equation fails to account for the milder slope of the real dependence, thereby significantly underestimating the charge at a low pH and overestimating it at a high pH.

The model of Tang et al.[10] also accounted for the Donnan effect by combining the Henderson-Hasselbalch equation with the Donnan partition coefficient. However, we have shown earlier in Ref.[21] that the ideal gas approximation for Donnan partitioning overestimates the strength of the Donnan effect, thereby overestimating the actual osmotic pressure. In Ref.[33] (Figure S2) we show that this is also true for the system considered here and that this difference is significant, both, below and above the counterion condensation threshold. In combination with the Gaussian approximation for chain elasticity, which is too weak at high stretching, the overestimated osmotic pressure resulted in a strongly exaggerated swelling, as compared to the experimentally determined values.[21]

Our simulations also confirmed that counterion condensation occurs in these systems only if they are sufficiently ionized, $\alpha > 0.5$. However, Tang et al.[10] neglected the Donnan effect when calculating α(pH) for their charge renormalization. Therefore, their renormalization was inconsistent with the calculation of net charge for the swelling. Consequently, it yielded a constant renormalization factor close to 1/6 at pH $\gtrsim 5$ whereas the ionization of the gel was changing significantly only at pH ≈ 6, followed by concomitant changes in the swelling. Ultimately, this constant renormalization factor yields a lower swelling degree of the gel, and thereby better agreement with the experiments, although it does not renormalize the charge in accordance with the calculated ionization degrees as a function of the pH. Indeed, a close inspection of Fig.9 of Ref.[10] reveals that the renormalized osmotic pressure as a function of the

pH has two inflection points: first at pH $\approx$ 5 and second at pH $\approx$ 6.5. It the authors of Ref.[10] had calculated the degree of ionization for charge renormalization in the same way as they calculated it for gel swelling, then the renormalization would yield a constant effective charge, as can be seen by substituting from Eq. 3 to Eq. 2:

$$q^{\mathrm{eff}}(\mathrm{pH}) = \frac{q_{\mathrm{max}} b_0}{2\lambda_{\mathrm{B}}} \quad \text{for} \quad \xi > 1, \tag{15}$$

Thus, the model of Tang et al. with correctly applied charge renormalization should predict that the swelling ratio does not change anymore, as soon as the counterion condensation threshold is reached. In our simulations, this threshold is reached at $\alpha \approx 0.5$ which corresponds to pH $\approx$ 6 according to Fig. 5a. However, Fig. 3 indicates that the swelling ratio continues to increase beyond this threshold, at a similar rate as before, until the full ionization of the gel is reached. This comparison indicates that although counterion condensation is present in these systems, the assumption that the effective charge is renormalized to the threshold value and the condensed counterions do not contribute to the osmotic pressure is not correct. We hypothesize that it is because the short polyelectrolyte chains, forming the gel network in salt solution, are too different from the infinite charged rod in a salt-free solution, for which the Manning theory has been derived.

If charge renormalization due to counterion condensation cannot explain the lower swelling of real hydrogels as compared to theoretical predictions, one should search for a different explanation. A plausible explanation has been suggested in our previous work,[21] where we have shown that the actual concentration of salt ions inside the gel is higher than that expected from the Donnan equation. In Ref.[33] (Figure S2) we show that this is true also for the gels simulated in our current work and that this difference cannot be explained by counterion condensation because it occurs well below the condensation threshold (pH $\approx$ 6). In addition, we have shown that Gaussian approximation to chain stretching is not sufficient for highly charged polyelectrolyte gels.[21] While the whole gel strands in the current system (neutral and acidic blocks

combined) are never near their maximum extension, the acidic blocks are significantly stretched in the high pH regime, in effect invalidating the use of the Gaussian chain stretching. As we have shown earlier, a much better functional form to use in this case is the Langevin function, which takes into account the finite extensibility of the chain.[13,21] Both these effects lead to a lower gel swelling than predicted by the ideal model, suggesting that an augmented model incorporating these effects might explain the lower swelling observed in the experiments by Tang et al.[10]. However, it is not clear yet, how these concepts should be applied to gels with a block-like structure. To do so, one would have to account for unequal stretching of the acidic and neutral blocks and for the inhomogeneous distribution of charged groups inside the gel. Therefore, incorporating these effects into a phenomenological model is beyond the scope of the current study.

4 Conclusion

We performed molecular simulations using a coarse-grained model of a weak polyelectrolyte hydrogel to investigate its swelling properties when immersed in salt solutions at various pH values and salt concentrations. The simulation model was designed to mimic the regular gels of tetra-PEG stars composed of alternating neutral and weakly acidic blocks, which have been investigated in recent experiments.[10] This setup enabled the first direct comparison of experiments with particle-based simulations of weak polyelectrolyte hydrogels without any adjustable parameters.

The simulated equilibrium swelling ratios as a function of pH values and salt concentrations in the supernatant solution were in good agreement with the experiments by Tang et al.[10] up to salt concentrations $c_{\mathrm{salt}} \lesssim 40\,\mathrm{mM}$ whereas some disagreement appeared at $c_{\mathrm{salt}} = 40\,\mathrm{mM}$. Additionally, simulations overestimated the swelling at low pH, when the gel was not ionized. We attributed these differences to the lack of chemical specificity of our gel model, which limits its predictive capabilities to states when electrostatic interactions dominate (intermediate and high ionization degrees, not too

high ionic strength).

We observed that the ionization of the gel as a function of pH was strongly suppressed as compared to the ideal Henderson-Hasselbalch result, in agreement with earlier studies on weak polyacid hydrogels.[9,12] Consequently, the effective pK_{A} of the hydrogel was shifted to higher pH values by almost two units. In analogy with our previous simulations of weak polyelectrolyte hydrogels[13], we showed that this shift originates from two effects: 1. the Donnan effect due to the Donnan partitioning of ions, which makes pH in the gel lower than pH in the reservoir; and 2. the polyelectrolyte effect due to electrostatic repulsion between ionized monomers in the gel. Unlike the previous study, our results showed that the shift in the pK_{A} of the gels composed of alternating acidic and neutral blocks is predominantly caused by the polyelectrolyte effect, whereas the Donnan effect is much weaker in this system. This behaviour is different from hydrogels with homogeneously distributed ionizable groups, in which the Donnan effect and the polyelectrolyte effect are comparable in magnitude, or the Donnan effect dominates.[13] By comparing how the radii of gyration of the neutral and ionizable blocks depend on the pH, we showed that the ionizable blocks considerably stretch as the pH is increased whereas the neutral blocks remain practically unaffected. This inhomogeneous swelling causes also an inhomogeneous distribution of ionizable groups in the gel which enhances the polyelectrolyte effect while simultaneously suppressing the Donnan effect.

Finally, we used our simulation results to test the hypothesis proposed by Tang et al. that the shift in the swelling of these hydrogels as a function of pH could be explained by charge renormalization invoking the Manning condensation of counterions. We identified a signature of counterion condensation only if the gels were sufficiently ionized. Nevertheless, the simulations showed that the gels continue to swell as the pH is increased even beyond the condensation threshold, whereas the charge renormalization predicts that their swelling should not change anymore. Therefore, the charge renormalization cannot explain the lower swelling observed in the experiments by Tang et al. Thus, one should search for alternative arguments to explain this observation,

such as the different stretching of neutral and charged blocks. Ultimately, we conclude that the model proposed by Tang et al. includes the influence of the Donnan and the polyelectrolyte effect on the ionization and concomitant swelling of their gels, and captures the qualitative behavior of the investigated gels. However, our simulations do not support their charge renormalization approach to explain lower swelling observed in experiment as compared to theoretical predictions.

5 Availability of Data

The simulation data and scripts are available free of charge from Ref.[33]

6 Acknowledgments

PK acknowledges the financial support of the Czech Science foundation, grant 21-31978J. CH acknowledges funds by the German Research Foundation (DFG) – grants No. 451980436 and No. 268449726. Parts of this work were also performed within the collaborative framework of the research unit *Adaptive Polymer Gels with Controlled Network Structure (FOR2811)*, funded by the German Research Foundation under No. 423435431. The authors acknowledge support by the state of Baden-Württemberg through bwHPC. We thank Jian Tang, Takuya Katashima and Takamasa Sakai for helpful discussion concerning the experimental system and for providing the experimental data.

References

(1) Zohuriaan-Mehr, M. J.; Omidian, H.; Doroudiani, S.; Kabiri, K. Advances in non-hygienic applications of superabsorbent hydrogel materials. *Journal of Materials Science* **2010**, *45*, 5711–5735, DOI: 10.1007/s10853-010-4780-1.

(2) Höpfner, J.; Klein, C.; Wilhelm, M. A Novel Approach for the Desalina-

tion of Seawater by Means of Reusable Poly(acrylic acid) Hydrogels and Mechanical Force. *Macromolecular Rapid Communications* **2010**, *31*, 1337, DOI: 10.1002/marc.201000058.

(3) Oh, J. K.; Drumright, R.; Siegwart, D. J.; Matyjaszewski, K. The development of microgels/nanogels for drug delivery applications. *Progress in Polymer Science* **2008**, *33*, 448–477, DOI: 10.1016/j.progpolymsci.2008.01.002.

(4) Hamidi, M.; Azadi, A.; Rafiei, P. Hydrogel nanoparticles in drug delivery. *Advanced Drug Delivery Reviews* **2008**, *60*, 1638–1649, DOI: 10.1016/j.addr.2008.08.002.

(5) Makino, K.; Idenuma, R.; Murakami, T.; Ohshima, H. Design of a rate- and time-programming drug release device using a hydrogel: pulsatile drug release from kappa-carrageenan hydrogel device by surface erosion of the hydrogel. *Colloids and Surfaces B-Biointerfaces* **2001**, *20*, 355–359, DOI: 10.1016/S0927-7765(00)00207-1.

(6) Tada, D.; Tanabe, T.; Tachibana, A.; Yamauchi, K. Drug release from hydrogel containing albumin as crosslinker. *Journal of Bioscience and Bioengineering* **2005**, *100*, 551–555, DOI: 10.1263/jbb.100.551.

(7) Wang, Q.; Li, S.; Wang, Z.; Liu, H.; Li, C. Preparation and Characterization of a Positive Thermoresponsive Hydrogel for Drug Loading and Release. *Journal of Applied Polymer Science* **2009**, *111*, 1417–1425, DOI: 10.1002/app.29026.

(8) Ricka, J.; Tanaka, T. Swelling of ionic gels: quantitative performance of the Donnan theory. *Macromolecules* **1984**, *17*, 2916–2921, DOI: 10.1021/ma00142a081.

(9) Philippova, O. E.; Hourdet, D.; Audebert, R.; Khokhlov, A. R. pH-responsive gels of hydrophobically modified poly (acrylic acid). *Macromolecules* **1997**, *30*, 8278–8285, DOI: 10.1021/ma970957v.

(10) Tang, J.; Katashima, T.; Li, X.; Mitsukami, Y.; Yokoyama, Y.; Sakumichi, N.; Chung, U.-i.; Shibayama, M.; Sakai, T. Swelling Behaviors of Hydrogels with Alternating Neutral/Highly Charged Sequences. *Macromolecules* **2020**, *53*, 8244–8254, DOI: 10.1021/acs.macromol.0c01221.

(11) Flory, P. J.; John Rehner, J. Statistical Mechanics of Cross-Linked Polymer Networks II. Swelling. *The Journal of Chemical Physics* **1943**, *11*, 521–526, DOI: 10.1063/1.1723792.

(12) Katchalsky, A.; Michaeli, I. Polyelectrolyte gels in salt solutions. *Journal of Polymer Science* **1955**, *15*, 69, DOI: 10.1002/pol.1955.120157906.

(13) Landsgesell, J.; Beyer, D.; Hebbeker, P.; Košovan, P.; Holm, C. The pH-Dependent Swelling of Weak Polyelectrolyte Hydrogels Modeled at Different Levels of Resolution. *Macromolecules* **2022**, *55*, 3176–3188, DOI: 10.1021/acs.macromol.1c02489.

(14) Schneider, S.; Linse, P. Swelling of cross-linked polyelectrolyte gels. *European Physical Journal E* **2002**, *8*, 457–460, DOI: 10.1140/epje/i2002-10043-y.

(15) Yan, Q.; de Pablo, J. J. Monte Carlo Simulation of a Coarse-Grained Model of Polyelectrolyte Networks. *Physical Review Letters* **2003**, *91*, 018301, DOI: 10.1103/PhysRevLett.91.018301.

(16) Edgecombe, S.; Schneider, S.; Linse, P. Monte Carlo Simulations of Defect-Free Cross-Linked Gels in the Presence of Salt. *Macromolecules* **2004**, *37*, 10089–10100, DOI: 10.1021/ma0486391.

(17) Yin, D.-W.; Yan, Q.; de Pablo, J. J. Molecular dynamics simulation of discontinuous volume phase transitions in highly-charged crosslinked polyelectrolyte networks with explicit counterions in good solvent. *The Journal of Chemical Physics* **2005**, *123*, 174909, DOI: 10.1063/1.2102827.

(18) Mann, B. A.; Holm, C.; Kremer, K. Swelling of Polyelectrolyte Networks. *The Journal of Chemical Physics* **2005**, *122*, 154903, DOI: 10.1063/1.1882275.

(19) Quesada-Pérez, M.; Ibarra-Armenta, J. G.; Martín-Molina, A. Computer simulations of thermo-shrinking polyelectrolyte gels. *The Journal of Chemical Physics* **2011**, *135*, 094109, DOI: 10.1063/1.3632051.

(20) Mann, B. A.; Lenz, O.; Kremer, K.; Holm, C. Hydrogels in Poor Solvents: A Molecular Dynamics Study. *Macromolecular Theory and Simulations* **2011**, *20*, 721–734, DOI: 10.1002/mats.201100050, Cover Issue.

(21) Košovan, P.; Richter, T.; Holm, C. Modeling of Polyelectrolyte Gels in Equilibrium with Salt Solutions. *Macromolecules* **2015**, *48*, 7698–7708, DOI: 10.1021/acs.macromol.5b01428.

(22) Landsgesell, J.; Hebbeker, P.; Rud, O.; Lunkad, R.; Kosovan, P.; Holm, C. Grand-Reaction Method for Simulations of Ionization Equilibria Coupled to Ion Partitioning. *Macromolecules* **2020**, *53*, 3007–3020, DOI: 10.1021/acs.macromol.0c00260.

(23) Sakai, T.; Matsunaga, T.; Yamamoto, Y.; Ito, C.; Yoshida, R.; Suzuki, S.; Sasaki, N.; Shibayama, M.; i. Chung, U. Design and fabrication of a high-strength hydrogel with ideally homogeneous network structure from tetrahedron-like macromonomers. *Macromolecules* **2008**, *41*, 5379, DOI: 10.1021/ma800476x.

(24) Manning, G. S. Limiting Laws and Counterion Condensation in Polyelectrolyte Solutions I. Colligative Properties. *The Journal of Chemical Physics* **1969**, *51*, 924–933, DOI: 10.1063/1.1672157.

(25) Deserno, M.; Holm, C.; May, S. Fraction of Condensed Counterions around a Charged Rod: Comparison of Poisson-Boltzmann Theory and Computer Simulations. *Macromolecules* **2000**, *33*, 199–206, DOI: 10.1021/ma990897o.

(26) Grest, G. S.; Kremer, K. Molecular dynamics simulation for polymers in the presence of a heat bath. *Physical Review A* **1986**, *33*, 3628–31, DOI: 10.1103/PhysRevA.33.3628.

(27) Weeks, J. D.; Chandler, D.; Andersen, H. C. Role of Repulsive Forces in Determining the Equilibrium Structure of Simple Liquids. *The Journal of Chemical Physics* **1971**, *54*, 5237, DOI: 10.1063/1.1674820.

(28) Kremer, K.; Grest, G. S. Dynamics of entangled linear polymer melts: A molecular-dynamics simulation. *The Journal of Chemical Physics* **1990**, *92*, 5057–5086, DOI: 10.1063/1.458541.

(29) Hockney, R. W.; Eastwood, J. W. *Computer Simulation Using Particles*; IOP: London, 1988.

(30) Deserno, M.; Holm, C. How to mesh up Ewald sums. I. A theoretical and numerical comparison of various particle mesh routines. *The Journal of Chemical Physics* **1998**, *109*, 7678, DOI: 10.1063/1.477414.

(31) Deserno, M.; Holm, C. How to mesh up Ewald sums. II. An accurate error estimate for the Particle-Particle-Particle-Mesh algorithm. *The Journal of Chemical Physics* **1998**, *109*, 7694, DOI: 10.1063/1.477415.

(32) Frenkel, D.; Smit, B. *Understanding Molecular Simulation*, 2nd ed.; Academic Press: San Diego, 2002; DOI: 10.1016/B978-0-12-267351-1.X5000-7.

(33) Beyer, D.; Košovan, P.; Holm, C. Electronic Supporting Information and Data for: Simulations explain the Swelling Behavior of Hydrogels with Alternating Neutral and Weakly Acidic Blocks. https://doi.org/10.18419/darus-2277.

(34) Weik, F.; Weeber, R.; Szuttor, K.; Breitsprecher, K.; de Graaf, J.; Kuron, M.; Landsgesell, J.; Menke, H.; Sean, D.; Holm, C. ESPResSo 4.0 – an extensible software package for simulating soft matter systems. *European Physical Journal Special Topics* **2019**, *227*, 1789–1816, DOI: 10.1140/epjst/e2019-800186-9.

(35) Manning, G. Limiting Laws and Counterion Condensation in Polyelectrolyte Solutions II. Self-Diffusion of the Small Ions. *The Journal of Chemical Physics* **1969**, *51*, 934–938, DOI: 10.1063/1.1672158.

(36) Naji, A.; Netz, R. R. Scaling and universality in the counterion-condensation transition at charged cylinders. *Physical Review E* **2006**, *73*, 056105, DOI: 10.1103/PhysRevE.73.056105.

(37) Nová, L.; Uhlík, F.; Košovan, P. Local pH and effective pKA of weak polyelectrolytes – insights from computer simulations. *Physical Chemistry Chemical Physics* **2017**, *19*, 14376–14387, DOI: 10.1039/c7cp00265c.
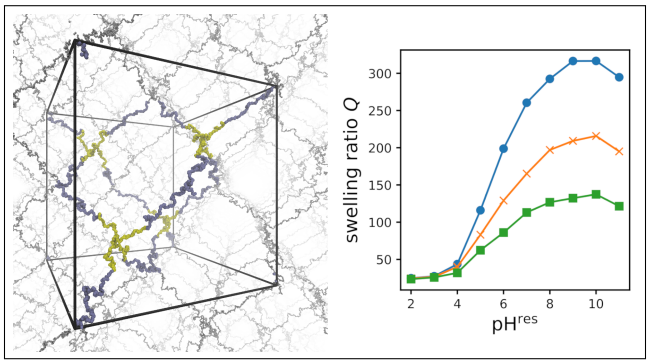
Graphical TOC Entry